Coral Reefs
DOI 10.1007/s00338-011-0749-z

REPORT

A simple approximation for larval retention around reefs

Paulina Cetina-Heredia · Sean R. Connolly

Received: 1 April 2010 / Accepted: 15 March 2011

Abstract Estimating larval retention at individual reefs by local scale three-dimensional flows is a significant problem for understanding, and predicting, larval dispersal. Determining larval dispersal commonly involves the use of computationally demanding and expensively calibrated/validated hydrodynamic models that resolve reef wake eddies. This study models variation in larval retention times for a range of reef shapes and circulation regimes, using a reef-scale three-dimensional hydrodynamic model. It also explores how well larval retention time can be estimated based on the "Island Wake Parameter", a measure of the degree of flow turbulence in the wake of reefs that is a simple function of flow speed, reef dimension, and vertical diffusion. The mean residence times found in the present study (0.48–5.64 days) indicate substantial potential for self-recruitment of species whose larvae are passive, or weak swimmers, for the first several days after release. Results also reveal strong and significant relationships between the Island Wake Parameter and mean residence time, explaining 81–92% of the variability in retention among reefs across a range of unidirectional flow speeds and tidal regimes. These findings suggest that good estimates of larval retention may be obtained from relatively coarse-scale characteristics of the flow, and basic features of reef geomorphology. Such approximations may be a valuable tool for modeling connectivity and meta-population dynamics over large spatial scales, where explicitly characterizing fine-scale flows around reef requires a prohibitive amount of computation and extensive model calibration.

Keywords Residence time · Island wake parameter · Larval retention · Connectivity · Coral reef · Eddies

Communicated by Environment Editor Prof. Rob van Woesik

Electronic supplementary material The online version of this article (doi:10.1007/s00338-011-0749-z) contains supplementary material, which is available to authorized users.

P. Cetina-Heredia (✉) · S. R. Connolly
School of Marine and Tropical Biology, James Cook University, Townsville, QLD 4811, Australia
e-mail: paulina.cetinaheredia@my.jcu.edu.au

S. R. Connolly
e-mail: sean.connolly@jcu.edu.au

P. Cetina-Heredia
School of Engineering and Physical Sciences, James Cook University, Townsville, QLD 4811, Australia

S. R. Connolly
ARC Centre of Excellence for Coral Reef Studies, James Cook University, Townsville, QLD 4811, Australia

Introduction

The dispersal of planktonic larvae influences many ecological and evolutionary phenomena. It affects the persistence of populations (James et al. 2002), the geographical distribution of species (Strathmann et al. 2002), population resilience to local disturbances (Steneck 2006; van Oppen and Gates 2006), population genetic structure (Hellberg et al. 2002), and potential for local adaptation (Done 1982; Willis and Oliver 1990). Therefore, an understanding of connectivity (i.e., the degree to which populations are linked through larval dispersal) is important for management and conservation in marine environments (Sale et al. 2005).

Connectivity is investigated using hydrodynamic models to simulate particle transport, and to quantify larval dispersal at specific geographical locations. Such models frequently

Published online: 19 April 2011

predict relatively high levels of connectivity among marine populations (e.g., Roberts 1997; Cowen et al. 2006). However, evidence of substantial self-recruitment exists across species with a broad range of life history traits (Swearer et al. 2002), and, in some cases, there is evidence that larval retention is likely to be higher than that predicted by hydrodynamic models (e.g., Gerlach et al. 2007). For strong swimmers, recent work suggests that larval behavioral strategies, such as oriented navigation, can enhance larval retention and facilitate self-recruitment (e.g., Kingsford et al. 2002). However, many other marine organisms have passive larvae for prolonged time (Nahas et al. 2003), and most marine invertebrates, such as corals, have weak swimming capabilities throughout their larval phase (Chia et al. 1984; Bradbury and Snelgrove 2001). Moreover, species whose larvae have strong swimming ability often take several days to begin swimming (e.g., Irisson et al. 2004). Thus, for the majority of marine organisms, local retention is likely to be substantially influenced by local-scale hydrodynamics, at least over the first few days of larval life. Hence, hydrodynamic models used to estimate dispersal need to characterize adequately the flow structures that induce larval retention around reefs.

In coastal waters, the interaction of currents with the ocean bottom provokes complex flows that in turn dictate particle trajectories. For instance, water flowing past reefs is associated with the formation of fronts, horizontal convergence, divergence, and upwelling. These types of flows, strongly influenced by vertical water movements, can distribute larvae in streaks (Wolanski and Hammer 1988; Wolanski et al. 1989) rather than uniformly across the surface (Parslow and Gabric 1989), and affect particle flushing times. Consequently, the effect of vertical flows is highly relevant for larval dispersal. Moreover, reefs induce friction, and thus turbulence (strong current velocity shear or linear stress); which leads to the formation of downstream reef-scale eddies. These eddies have been observed to affect larval distributions (Wolanski et al. 1989; Willis and Oliver 1990; Burgess et al. 2007). Lee eddies can promote larval retention by recirculating larvae or accumulating them in regions where secondary convergent flows occur (Wolanski et al. 1996; Sponaugle et al. 2002). However, such eddies can also accelerate transport across the wake if larvae become entrained in the eddy and travel along its edge where velocities are greater (Sandulescu et al. 2006), or they can enhance larval dispersion by the straining motions of the eddies (Signell and Geyer 1991). Hence, to accurately simulate larval transport in shallow waters, models must not only account for three-dimensional hydrodynamics that solve the vertical flow structure, but also utilize a spatial resolution fine enough to depict the effect of complex bathymetry, such as around reefs (Wolanski 1993; Marinone 2006) on the horizontal flow structure.

In order to incorporate a reef-scale (hundreds of meters) spatial resolution, and capture the effects of three-dimensional flows in hydrodynamic models, substantial computational power is required, even at the scale of individual reefs. However, larval dispersal can occur over great distances (e.g., tens or even hundreds of kilometers; James et al. 2002; Cowen et al. 2006); therefore, dispersal models must cover large geographical areas. These twin requirements present a substantial logistical challenge for the simulation of dispersal patterns. One approach has been to use high resolution models for regions of shallow waters (e.g., around reefs), nested within coarse resolution models that cover broad geographical areas (e.g., Tang et al. 2006). Most recently, models that allow changes in resolution within the same grid have been developed (Legrand et al. 2006). However, these approaches involve extensive model calibration, which in turn, requires observations at many different locations. Alternatively, advection–diffusion approximations that parameterize smaller-scale flows (Paris and Cowen 2004; Marinone et al. 2008) can be implemented in coarse resolution models that allow a wide geographical coverage. However, diffusion is highly spatially and temporally variable in the ocean (Visser 1997), and thus extensive calibration with observations is required to adequately characterize the flow structure found in the vicinity of reefs when this approach is employed.

In this study, we explore a new approach to overcoming the logistical problems associated with modeling reef-scale flow features in a metapopulation context, by investigating how well the larval retention simulated by a reef scale three-dimensional model can be estimated with very simple functions that incorporate effects of reef dimension, flow velocity, and bottom friction scales on retention times. In order to determine how reef-scale circulation features affect larval retention, a high-resolution ($\sim$100 m), three-dimensional hydrodynamic model was used to estimate larval retention by reefs with different shapes and sizes, under a range of circulation regimes (i.e., under different combinations of unidirectional and tidal flow intensities).

To approximate the effects of reef dimension, flow velocity and bottom friction scales on retention time, we examined a dimensionless number, termed the "Island Wake Parameter" that characterizes the flow behind topographic outcrops in shallow waters (Wolanski et al. 1984). Analogous to the Reynolds number, the Island Wake Parameter indicates whether the flow past an obstacle has turbulent characteristics, such as whether eddies are expected to form behind the obstacle and how stable these flow structures are (Tomczak 1988; Barton 2001). For Island Wake Parameter values on the order of unity, stable eddies are expected to form behind the obstacle. Smaller values are predicted to produce laminar flow. Larger values are predicted to lead to eddy formation, detachment, and

dissipation. In previous work, this number has proved successful at predicting these qualitative features of the wake (Neill and Elliott 2004; Pattiaratchi et al. 1986). The present study tests whether differences among reefs in the Island Wake Parameter can explain associated differences in larval retention times induced by a particular circulation regime, and whether the relationship between retention time and Island Wake Parameter varies predictably among circulation regimes. This approach offers the potential to estimate the larval retention induced by three-dimensional, reef-scale flow structure in a simple and tractable way, without the need to explicitly model that flow structure. Moreover, such simple approximations potentially can be applied even at locations where hydrodynamic models cannot readily be implemented, due to insufficient oceanographic data.

Methods

The Island Wake Parameter

The Island Wake Parameter, I, is the ratio of advective to frictional terms, relevant to the flow past an obstacle in shallow waters. In this type of environment, bottom drag is the primary source of velocity shear (Dong and McWilliams 2007). Bottom drag causes a stress boundary layer that generates turbulence and vertical momentum transfer. Consequently, the pertinent frictional terms are the vertical turbulent diffusion coefficient K_z, and the water depth H. K_z represents the vertical momentum transfer due to turbulence, it allows the development of eddies and is expected to influence their persistence (Moum et al. 1988). The advection term is determined by the acceleration that the particles experience when they deviate from their intended path as they approach the obstacle. This term is related to the velocity, V, of the current that impinges upon the obstacle, and the width, W, of the obstacle. Hence, the Island Wake Parameter is given by:

$$I = \frac{VH^2}{K_z W} \tag{1}$$

Although the expression for the Island Wake Parameter is simple, many of the constituent terms are not constant. For instance, the velocity upstream of an obstacle may vary over time and space. For consistency, in this study, V was determined as the maximum velocity over time found within the region upstream of the obstacle in each simulation. H is constant (50 m) for all simulations. This depth is within the range of depths around inner and middle shelf reefs along the Great Barrier Reef (GBR). W is the dimension of the reef perpendicular to the incoming flow.

In the field, vertical diffusion (K_z) is highly spatially and temporally variable (even within individual eddies), and is time-consuming to measure (e.g., Bricker and Nakayama 2007). Using such measurements when applying Eq. (1) would defeat the purpose of a simple approximation based on measuring easily obtainable quantities, such as reef dimensions. Previous uses of the Island Wake Parameter approximate K_z by applying Taylor's theory (1954), according to which vertical diffusion is proportional to the drag coefficient, flow velocity, and depth. However, this approximation is problematic because the Island Wake Parameter becomes independent of velocity. Instead, we use a background vertical diffusion specified in the simulations (0.01 m s^{-1}). This quantity represents the extent of vertical momentum transfer in the ocean's interior, and it is a lower bound on the total vertical diffusion, which is:

$$K_z = K_b + \alpha\mu H(1 + 3.33R_i)^{-3/2} \tag{2}$$

where μ is the maximum of the surface and bottom friction velocities, α is a constant, and R_i is the Richardson number, dependent on the vertical stratification and vertical velocity shear (Herzfeld et al. 2006).

Hydrodynamic and particle tracking model

The Sparse Hydrodynamic Ocean Code (SHOC) was used to compute velocity fields and track individual passive particles. SHOC was developed by the Environmental Modeling group at the Commonwealth Scientific and Industrial Research Organization (CSIRO), and was previously termed the Model for Estuaries and Coastal Oceans (MECO) (Parslow et al. 2001; Wolanski et al. 2003). It has proved useful for investigating circulation in coastal areas (Walker 1999), larval transport in estuaries (Condie et al. 1999) and more recently, across and along shelf connectivity in Western Australia (Condie and Andrewartha 2008). Briefly, SHOC is a finite difference model based on the three-dimensional equations of momentum that uses the hydrostatic and Boussinesq approximations. The equations are solved in an Arakawa C grid, and are written for a curvilinear orthogonal horizontal mesh and a set of chosen "z" coordinates in the vertical, Herzfeld et al. (2006). The turbulence closure scheme implemented was the k-ε (Burchard et al. 1998), and a Lagrangian particle tracking algorithm contained within SHOC, was used to obtain simultaneously the velocity field and the particle location for the entire simulation time.

A common grid with nine depth layers was used for the simulations. Given that particles were initially located above the reef, and the reef surface was 5 m underwater, a higher vertical resolution (0.5 m) near the surface, and a coarser vertical resolution (5 m) in the rest of the water column was adopted for all simulations.

Research on the nature of lee reef eddies, including modeling (Black and Gay 1987), remote sensing, and in situ observations (Wolanski et al. 1984), have reported that the size of these circulation features is 1–2 times the size of

the reef's side perpendicular to the incoming current. In order to capture the dynamics of a vortex, a minimum of three grid points across the gyre are necessary. Because the simulations were run for reefs with widths ranging from 600 to 3,600 m, a spatial resolution of ~200 m was used to ensure a minimum of three grid points across the smallest of the expected eddies. Every time step, the particles were advected with the velocity explicitly solved by the hydrodynamic model plus a random diffusion velocity. This diffusion velocity was determined by drawing a random number from a Gaussian distribution with mean zero and standard deviation equal to the diffusion coefficient relevant to spatial scales smaller than the grid size, that is ~0.09 m^2 s^{-1} (Okubo 1971).

Our use of a constant resolution, allowed implementing the same horizontal diffusion coefficient to induce particle diffusion caused by sub-grid flows in all simulations. However, this approach does imply more grid cells behind larger reefs than behind small reefs, and thus potentially poorer resolution of eddy structure behind smaller reefs. However, preliminary simulations with finer horizontal resolution resulted in retention times within 3% of one another, even for smaller reefs, which suggests that scaling grid cell size to reef size would have had a negligible effect on results.

For each simulation, 10^4 passive particles were released randomly distributed in the water column above the reef. The time, relative to the tidal cycle, at which particles were released had a negligible effect on particle retention; therefore particles were released at time zero.

Scenarios

This study examines how well *I* captures the characteristics of the flow past obstacles and can be used as a statistical predictor of residence times. As noted above (Eq. 1), *I* is a function of: the reef dimension perpendicular to the incoming flow, the flow magnitude and the vertical diffusion coefficient. Therefore, to determine the relationship between *I* and residence time, this study analyses simulations for a range of reef shapes, reef dimensions, and flow speeds generated by different combinations of unidirectional and tidal flows of different intensities.

Rectangular and triangular reef morphologies were used, because they resemble common reef shapes along the GBR; kidney-shaped reefs also were examined to incorporate the effects of a semi-enclosed central reef lagoon on larval retention (Fig. 1). For each of these shapes, length and width dimensions were varied in order to encompass a wide spectrum of geometries. In total, we ran simulations for twelve rectangular, six triangular, and eight kidney reefs (see Table 1). Bathymetry was uniform, with reefs submerged 5 m from the surface, rising straight from a 50 m flat bottom.

Because *I* incorporates only the upstream obstacle flow intensity, we first implemented a unidirectional flow. Simulations were run for all rectangular reefs, for a range of intensities (~0.06–0.77 m s^{-1}). For each flow intensity, the relationship between *I* and mean retention time was quantified as described under *Methods*: "Statistical analysis", below. Estimated parameters characterizing this relationship were compared across flow intensities, to determine whether and how the functional relationship between *I* and residence time varied. To determine whether these relationships were robust to reef shape, simulations for the triangular and kidney shapes were run for two of these flow intensities, which we term "weak" and "strong", *wU* and *sU*, respectively, where *w* denotes weak, *s* denotes strong, and *U* denotes unidirectional flow.

A unidirectional flow resembles a dominant alongshore low frequency current (e.g., Eastern Australian Current, EAC). However, circulation in reefs systems can also be influenced by high frequency tidal currents. It is therefore important to test the effect of such flows on *I* and its functional relationship with residence times. Therefore, circulation regimes that consisted of both, a unidirectional flow, plus a perpendicular tidal flow were implemented. Although tidal currents are not always perpendicular to low frequency currents, this is particularly common along the Eastern Australian coast where the GBR is located (Wolanski and Pickard 1985). Moreover, because *I* implicitly accounts only for flow in one direction, implementing tidal currents flowing perpendicularly to such flow provides a particularly stringent test of the robustness of *I* as a statistic describing circulation around reefs. Three different scenarios combining unidirectional and tidal flows were implemented: weak unidirectional and weak tidal (*wUwT*), weak unidirectional and strong tidal (*wUsT*), and strong unidirectional and strong tidal (*sUsT*).

Boundary forcing

The grid is oriented in a North–South East–West direction, has dimensions of 80 by 45 grid cells (16 by 9 km), and has four open boundaries through which we forced the model. The reefs were located seven grid cells south of the northern boundary, and at least twenty grid cells away from the east and west boundaries. Simulations using alternative distances indicated that this was far enough from the domain limits to avoid any effect of the boundaries on particle transport. To simulate the unidirectional flow scenarios, we constrained the current magnitudes at the south and north boundaries to remain constant in both magnitude and southward direction. To model effects of flow intensity, these current magnitudes were constrained to specific values ranging between 0.05 and 0.65 m s^{-1}.

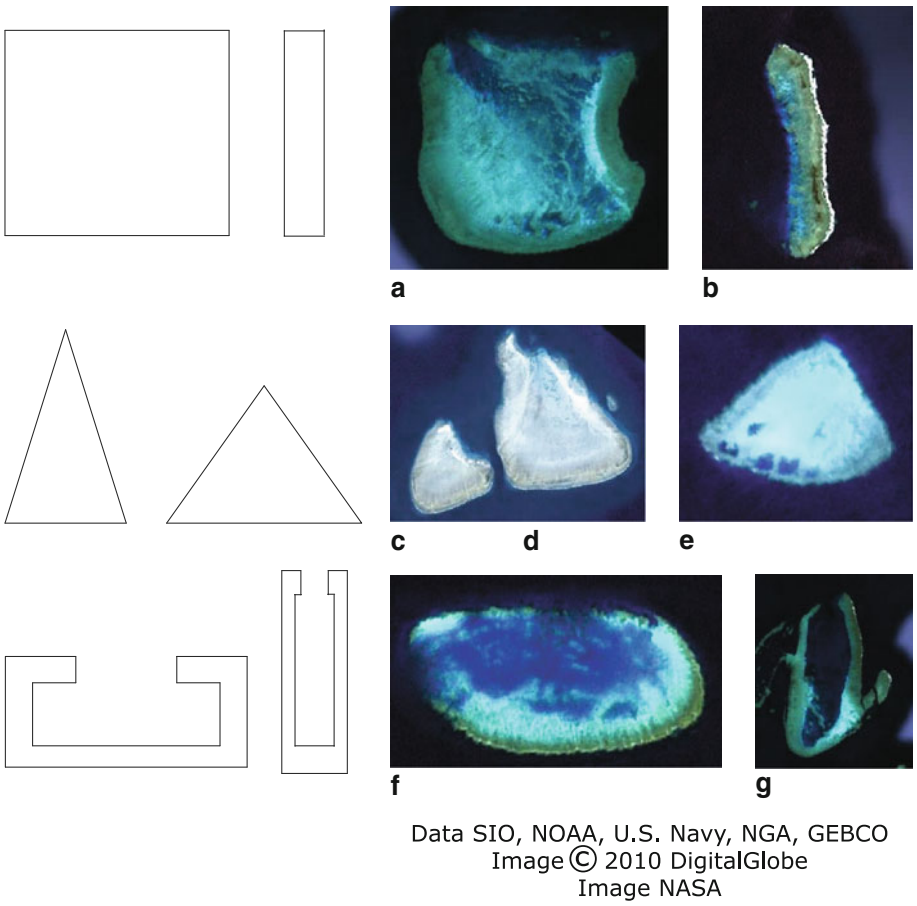

Fig. 1 Modeled reef geometries and reef images along the GBR from Google Earth, examples for: **a** and **b** *rectangle*, **c**, **d** and **e** *triangle*, and **f** and **g** kidney shaped reefs. The reef images are oriented parallel to the coastline (main direction of the EAC). Their longitude and latitude are: (a) 149° 49′E, 20°04′S (b) 145° 45′E, 15° 16′S (c) 145° 20′E, 14° 47′S (d) 145° 20′E, 14° 45′S (e) 150° 50′E, 21° 09′S (f) 147° 03′E, 18° 37′S, and (g) 150° 19′E 20° 06′S

This generated maximum flow magnitudes between 0.065 and 0.77 m s^{-1} within the model domain, consistent with the range of reported magnitudes for low frequency currents along the GBR (Wolanski and Pickard 1985). For simulations investigating effects of reef shape, and presence of tidal flows, the "weak" and "strong" unidirectional flow scenarios corresponded to southward magnitudes of 0.05 and 0.12 m s^{-1} at the boundaries (generating maximum flows of 0.11-0.51 m s^{-1} within the model domain). To implement the tidal flows, we forced the east and west boundaries with synthetic sea level elevation time series (e.g., Wolanski et al. 1989). Specifically, the sea level time series were generated as the sum of diurnal and semidiurnal harmonics with amplitudes that would generate maximum tidal current magnitudes of 0.16 m s^{-1} and 0.44 m s^{-1} for the weak and strong tidal flow scenarios, respectively. This encompasses a range of tidal current magnitudes which are consistent with observational studies along the GBR (Griffin et al. 1987). The necessary forcing to generate a strong unidirectional flow provoked simultaneous strong tidal flows. Hence, it was not feasible to recreate the effect of a strong unidirectional flow coupled with a weak tidal flow.

Particle abundance and residence time

For all simulations, each 3D particle position was recorded every 30 min for the duration of the simulation (10–15 days). Particles were designated as "retained" if they remained within a region where they could be either entrained in a wake eddy, and ultimately brought back to the reef, or to be advected back over the reef after a tidal reversal. We delimited the retention area by counting 18 grid cells (the dimensions of the largest observed lee eddy) to the south of each simulated reef. Simulations indicated that eastward and westward displacement of eddies by tidal flows were of similar magnitude, so we extended the retention area east and west of the reef edges by 18 cells also. We adopted this approach, rather than scaling retention area to expected eddy size separately for each reef, to make our test of I more conservative. Specifically, smaller reefs tend to have larger I (Eq. 1). Using a smaller retention area would also tend to reduce retention times, and thus potentially amplify the expected negative relationship between I and mean retention time. In all simulations, all larvae that left the retention area did so past the southern boundary. This indicates that the designated retention area

Table 1 Percent of particles remaining inside the retention area 12 h, 2 and 4 days after release for each reef and circulation regime

	Reef dimensions		Time													
	Length (km)	Width (km)	12 h					2 days					4 days				
			Circulation regime														
			wU	*wUwT*	*wUsT*	*sU*	*sUsT*	*wU*	*wUwT*	*wUsT*	*sU*	*sUsT*	*wU*	*wUwT*	*wUsT*	*sU*	*sUsT*
Rectangle	4.0	0.6	100	99.98	99.95	50.26	30.80	0.03	0.03	0.32	0.03	0.03	0.03	0.03	0.03	0.03	0.03
	4.2	0.6	99.81	99.74	99.82	63.44	55.18	0.13	0.59	1.36	0.01	0.01	0.01	0.01	0.02	0.01	0.01
	3.0	0.6	99.99	99.98	99.99	71.08	66.68	0.28	0.28	1.72	0.01	0.01	0.01	0.01	0.01	0.01	0.01
	1.6	0.8	99.99	99.96	99.92	71.24	49.73	1.55	0.86	0.77	0	0	0	0	0	0	0
	0.8	0.8	99.99	100	99.96	82.21	53.12	11.46	5.17	1.25	0.37	0.07	0.05	0.02	0.01	0	0.02
	2.0	1.0	100	100	100	90.51	84.24	19.38	12.65	8.34	2.36	0.04	0.43	0.02	0.08	0.10	0
	1.4	1.0	100	99.97	99.93	89.87	75.82	19.14	14.42	4.81	2.47	0.18	0.39	0.08	0.01	0.04	0.01
	1.2	1.2	100	99.99	99.97	93.54	74.32	25.85	23.30	5.26	10.03	0.38	1.97	1.00	0.04	0.54	0.01
	1.0	1.4	100	100	99.96	95.46	80.98	45.09	40.26	5.25	25.24	0.84	9.07	5.92	0.05	4.14	0
	1.6	1.6	100	100	99.99	95.02	84.06	41.87	35.74	20.11	22.24	1.22	9.61	4.44	3.03	4.04	0.02
	1.0	2.0	100	100	99.96	98.44	89.31	68.77	57.89	9.77	51.56	1.03	31.21	24.67	0.26	20.82	0.02
	1.0	2.8	100	99.99	99.97	99.62	94.61	79.59	61.17	17.92	55.82	0.83	46.29	30.56	2.89	34.29	0
Kidney	2.8	1.0	100	99.99	99.97	85.08	80.02	19.22	16.45	17.31	3.86	3.68	5.24	5.80	6.90	1.02	0.65
	2.0	1.0	99.94	99.89	99.98	80.47	66.27	18.12	14.17	14.89	3.97	1.82	4.83	4.42	4.50	0.72	0.28
	1.4	1.0	100	100	99.98	90.25	86.00	22.91	19.40	11.52	4.42	19.95	4.81	3.81	3.08	0.67	18.00
	1.0	1.4	100	100	99.98	96.51	86.00	61.13	56.84	29.00	40.30	19.95	32.11	29.00	19.37	22.16	18.00
	1.0	2.0	100	100	99.98	98.74	90.89	74.09	66.33	20.66	51.07	3.35	40.33	33.58	2.85	20.34	0.13
	1.0	2.8	100	100	100	99.75	96.45	86.88	75.88	44.35	66.23	27.72	64.03	53.51	29.63	49.57	26.15
	1.4	2.8	100	100	99.99	99.41	96.35	76.16	65.94	47.18	47.00	11.81	48.73	39.30	20.31	27.27	0.76
	1.8	3.6	100	100	99.99	99.18	94.68	78.16	68.81	35.20	52.86	4.73	48.12	40.20	8.87	28.47	0.18
Triangle	1.0	1.0	100	99.99	99.95	88.34	71.16	22.30	7.28	3.08	5.82	0.03	0.86	0.01	0.01	0.24	0.01
	1.4	1.6	100	99.98	99.91	92.82	76.40	44.77	24.23	5.42	25.22	0.09	10.58	0.98	0.02	4.54	0.01
	1.4	1.2	100	100	99.94	97.29	75.13	53.39	28.08	1.30	31.77	0.19	14.97	1.62	0.01	6.85	0.01
	2.0	1.4	100	100	99.99	98.53	74.88	62.65	38.92	2.76	47.07	0.24	28.93	9.70	0.02	18.78	0.02
	2.2	1.2	100	99.99	99.77	98.79	72.50	73.42	39.02	1.94	53.13	0.24	38.18	9.86	0.01	24.57	0.03
	3.4	1.0	100	100	100	100	98.95	86.59	64.88	22.45	66.58	1.38	54.18	24.78	2.68	44.22	0.04

was sufficiently large to account for any East–West tidal recirculation or northward diffusion of larvae and that extending the area to the north, east, or west of the reef any further would have had no effect on the results.

The number of particles inside the retention area was calculated to obtain particle abundance over time, and the time at which each particle was advected out of this area was recorded. Mean residence time is the average time at which particles were flushed from the retention area. To evaluate how the potential for local self-recruitment varied among reef shapes, reef dimensions, and circulation regimes, we also estimated the percentage of larvae remaining inside the reef vicinity after 12 h, 2, and 4 days. We chose 4 days as our maximum for this calculation because it is approximately the time required for broadcast-spawning corals to become competent to settle (Nozawa and Harrison 2008; Glimour et al. 2009). It is also approximately the time required for some fish to develop swimming ability (Irisson et al. 2004). Similarly, broadcast-spawned sponge larvae take between 12 and 54 h, to metamorphose and settle (Leys and Degnan 2001; Whalan et al. 2008).

Statistical analysis

$I < 1$ represents laminar flow $I \sim 1$ the formation of eddies that remain attached downstream the obstacle, and $I > 1$ the formation and detachment of eddies. This could provoke shorter residence times as I increases above 1. Therefore, to quantify how *well* I predicts residence times, we used a power-law relationship, modified to include an offset term:

$$R = aI^b + c \quad (3)$$

where R denotes residence time, I the Island Wake Parameter, and a, b, and c are fitted regression parameters.

b represents the steepness of the relationship between the residence time and the Island Wake Parameter, as I increases from low values and the flow changes from friction-dominant to advection-dominant. We expected this parameter to be negative (i.e., shorter residence times for larger values of I). Consequently, the first term in Eq. (2) should approach zero as I increases, and thus c represents an asymptotic minimum possible residence time (i.e., residence time as I approaches infinity). The existence of such a minimum is plausible on physical grounds because, as friction becomes overwhelmed by advection, at very large I values some minimum time may still be required for larvae to be flushed from the retention area. To test for such a minimum, we also fit regression models where c was fixed at zero, and only a and b were estimated; where likelihood ratio tests did not indicate significant support for the full three-parameter model, we used the simpler model. The parameter a represents the additional retention due to the presence of an ideal stable eddy; that is, $a + c$ is the predicted retention time when $I = 1$. I was log-transformed for analysis, to homogenize residual variances.

First, regressions were conducted separately for all rectangular reefs and each unidirectional flow speed, to determine whether the relationship between retention time and I varied systematically among unidirectional flow intensities (i.e., different a, b, and c parameters for each unidirectional flow regime). A regression was also conducted by pooling the data across unidirectional flow intensities (i.e., a single a, b, and c parameter applies to all unidirectional flows). We used a likelihood ratio test to determine whether the model with separate parameters was significantly better than the pooled model.

Secondly, we conducted regression and likelihood ratio test to determine how well Eq. (3) predicted retention time for rectangular reefs under the flows with and without tides, and whether there were significant differences in parameters a, b, and c depending on the tidal regime.

Thirdly, to test the effect of reef shape on the relationship between the residence time and I, regressions were conducted for each reef shape separately (i.e., different parameters a, b, and c for the rectangular, triangular, and kidney shaped reefs), and compared with a regression in which all reef shapes were pooled in a single analysis. A likelihood ratio test was used for model selection between the pooled model and the models with different regression parameters for each reef shape.

Finally, we pooled the results for all simulations (all reef shapes, unidirectional flow intensities, and tidal regimes) in a single regression to determine how well a single fit of Eq. (3) could approximate retention time across the entire set of simulations.

Results

Island Wake Parameter and residence time values

I ranged between 0.6 and 31, implying a range of flow structures without lee eddies, to those with unstable eddies. Comparisons between I and the corresponding velocity and vorticity fields showed that $I \sim 1$ values were associated with persistent eddies behind the obstacle (Fig. 2a), and large $I > 1$ values were consistently associated with strong vorticity gradients (Fig. 2b, c).

Overall, mean residence times obtained from the simulations varied by approximately an order of magnitude: from 0.48 to 5.74 days. After 12 h, the majority of the particles (50–100%) are retained at all but one reef, regardless of the circulation regime. By 4 days, most particles had been flushed away from most of the reefs but with considerable variation (Table 1); for narrow rectangular reefs, <1% of particles remained in the retention area regardless of circulation regime; for kidney-shaped reefs, retention time was substantially greater, ranging up to 64% of particles remaining, and for triangular reefs, retention times varied widely, from <0.1% retained particles for narrow reefs under strong flows, to >50% for wide reefs in weak flows.

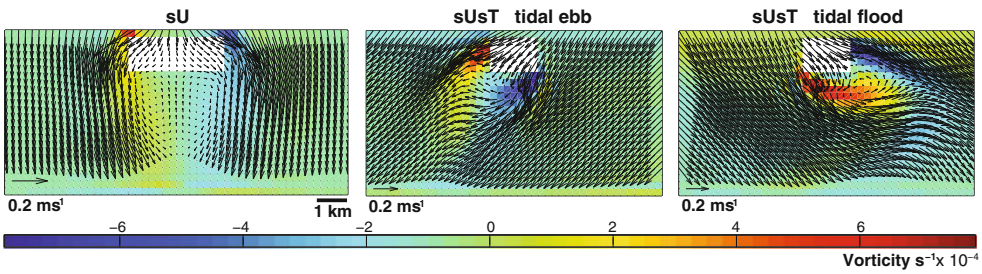

Fig. 2 Top view snapshots of the velocity field (*arrows*) and vorticity or horizontal velocity shear (color scale) for different flow regimes: **a** strong unidirectional (*sU*), **b** strong unidirectional strong tidal (*sUsT*) at ebbing time, and **c** strong unidirectional strong tidal (*sUsT*) at flooding time. Each panel shows the retention area and reefs are shown in *white*

The scaling of the mean and variance of residence time, calculated over the whole simulation time period (10–15 days), was fairly similar across reef shapes and sizes, and among circulation regimes (Electronic Supplemental Material, ESM, Fig. A1), suggesting that differences in mean retention time provide a good description of overall differences in retention patterns among reefs and circulation regimes. Therefore, the analyses below focus on mean retention time as the response variable for identifying the effects of reef size, shape, and of circulation regime, on larval retention.

Relationship between residence time and Island Wake Parameter

The wake structure, characterized by *I,* on particle distribution was evident (Fig. 3). Strong statistical relationships were found between residence time and *I* in all the analysis reported below. All regressions were statistically significant, and explained >80% of the variation in the simulated mean retention times. For the analysis of different unidirectional flow speeds, regressions account for a large proportion of the variability shown in the data (84-92%). The likelihood ratio tests showed no significant support for the inclusion of parameter *c*. Although parameters *a* and *b* appear to increase slightly toward an asymptote across the examined flow speeds (ESM, Table A1), the changes are small, so the likelihood ratio test supports the pooled model, in which a single set of regression parameters describes the relationship across all flow speeds ($G = 27.9$, critical $\chi^2_{(18,0.05)} = 28.86$, $P = 0.06$ Fig. 4; Table 2). The relationship between *I* and residence time remains excellent for circulation regimes with tidal flows (ESM, Table A2). Parameter *c* is significantly different from zero when weak tidal flows are present (ESM, Table A2). Again, however, a likelihood ratio test favors the pooled model, where a single set of model parameters applies across all

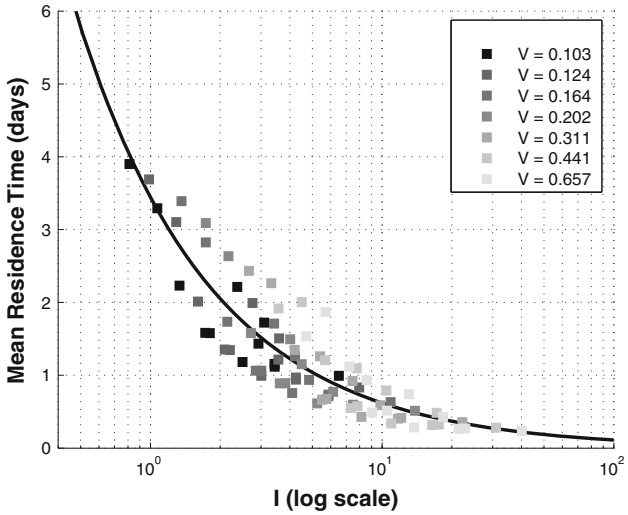

Fig. 4 Relationship between the Island Wake Parameter (*I*) and mean residence time from the unidirectional flow simulations. Each *square* represents a particular reef size, and each shade of grey corresponds to a particular flow intensity. The line is the regression for the rectangular reefs with all unidirectional flow intensities pooled

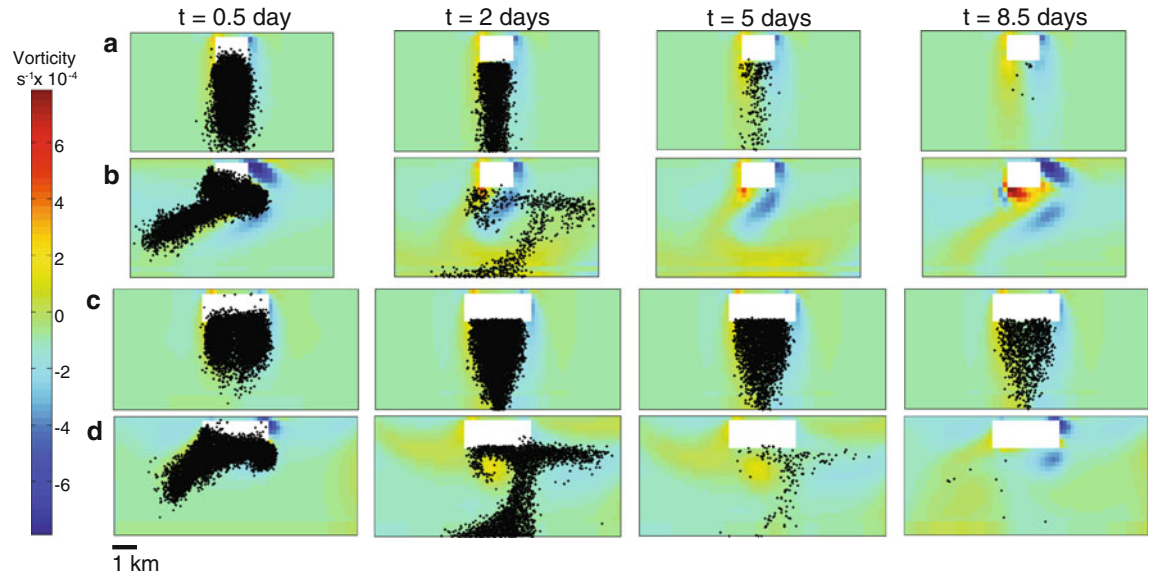

Fig. 3 Top view snapshots of particle distribution (*black dots*) and vorticity field over times ($t = 0.5$, 2, 5, and 8.5 d) for: **a** reef A under strong unidirectional flow (*sU*) **b** reef A under strong unidirectional and weak tidal flow (*sUwT*), **c** reef B under strong unidirectional flow (*sU*), and **d** reef B under strong unidirectional weak tidal flow (*sUwT*). Each *panel* shows the retention area and reefs are shown in *white*

Table 2 Regression parameters with 95% confidence bounds, coefficient of determination (R^2), F statistic, P values, and likelihood ratio (G) for the favored regression models between the Island Wake Parameter (I) and Residence time

Circulation regime	Reef shape	G	c (95% cb)	a (95% cb)	-b (95% cb)	R^2	F	P value
All unidirectional flow speeds pooled	Rectangular	0.0024	NA	3.44 (3.15 3.73)	0.74 (0.66 0.74)	0.81	1680	<0.001
wU/sU/wUwT/wUsT/sUsT pooled	Rectangular	11.57	0.62 (0.38 0.87)	2.64 (2.31 2.98)	1.11 (0.79 1.42)	0.82	128	<0.001
wU/sU/wUwT/wUsT/sUsT pooled	All	5.11	0.61 (0.35 0.86)	3.12 (2.83 3.50)	3.49 (1.20 0.96)	0.82	290	<0.001
All unidirectional flow speeds/wUwT/wUsT/sUsT pooled	All	1.61	NA	3.75 (3.57 3.92)	0.81 (0.75 0.88)	0.82	891	<0.001

$G > 3.841$ indicates statistically significant support for a non-zero value of c. F statistics indicated that all reported regressions were highly statistically significant ($p \ll 0.01$ in all cases)

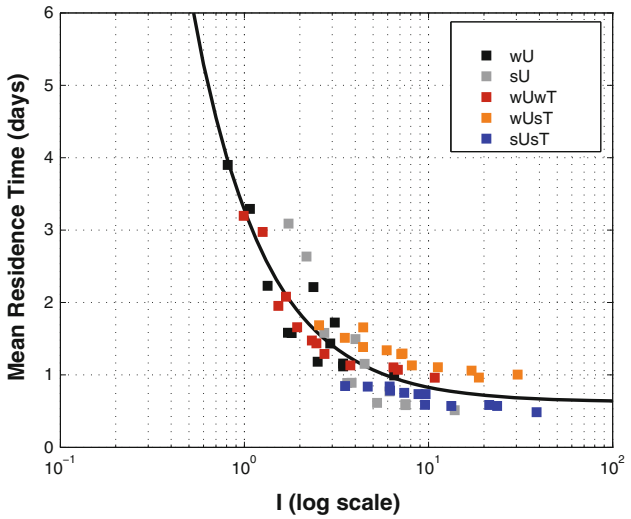

Fig. 5 Relationship between the Island Wake Parameter (I) and mean residence time showing the effects of tidal regime. Each square represents a particular reef size, and each color corresponds to a particular flow regime. The line is the regression for the rectangular reefs pooled across circulation regimes: weak unidirectional (*wU*), strong unidirectional (*sU*), weak unidirectional and weak tidal (*wUwT*), weak unidirectional and strong tidal (*sUwT*), and strong unidirectional and strong tidal (*sUsT*)

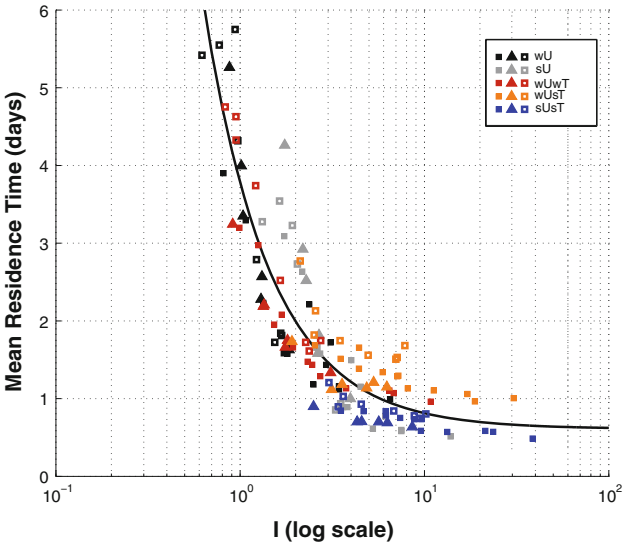

Fig. 6 Relationship between the Island Wake Parameter (I) and mean residence time, showing the effects of reef shape: *Square* indicate kidney-shaped reefs, *Filled square* indicate rectangular reefs, and *Filled triangle* indicate triangular reefs. Each color corresponds to a particular flow regime. The line is the regression pooled across reef shapes (rectangles triangles, and kidneys) and across circulation regimes: weak unidirectional (*wU*), strong unidirectional (*sU*), weak unidirectional and weak tidal (*wUwT*), weak unidirectional and strong tidal (*sUwT*), and strong unidirectional and strong tidal (*sUsT*)

tidal regimes ($G = 5.11$, critical $\chi^2_{(7,0.05)} = 14.07$, $P = 0.65$) (Fig. 5; Table 2). Differences between reef shapes modify the intensity of changes in residence times due to changes in I. Specifically, the steepness, or parameter b, is smallest for kidney reefs, and largest for triangular shaped reefs (ESM, Table A3). Again, however, a likelihood ratio test favors a single set of regression parameters across all shapes ($G = 14.38$, critical $\chi^2_{(8,0.05)} = 15.50$, $P = 0.07$) (Fig. 6, Table 2).

Finally, a single regression between I and residence times, pooling all the circulation regimes and reef shapes, also provides an excellent fit, explaining 82% of the variation in retention time (Fig. 7; Table 2).

Discussion

Island wake parameter, qualitative flow characteristics, and residence time

This study confirms that the ratio of advection to bottom friction, as expressed by I, characterizes qualitatively the flow structure behind topographic mounts in shallow waters. The Island Wake Parameter values and associated flow fields obtained in this study are consistent with theoretical predictions. I values close to unity were found for wide reefs under weak and strong unidirectional flows and

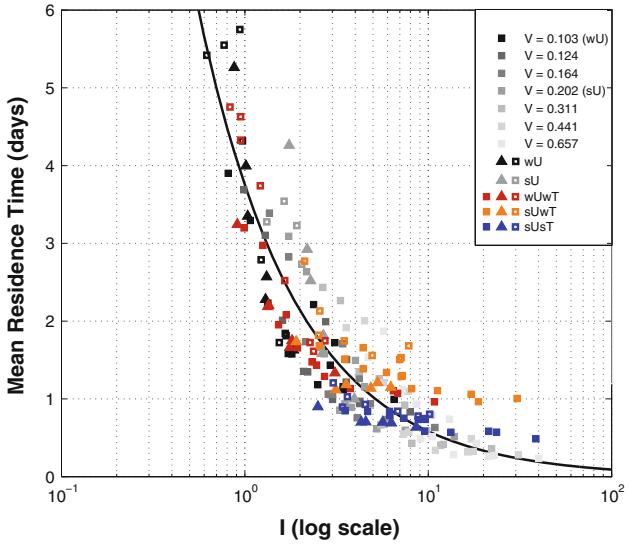

Fig. 7 Relationship between the Island Wake Parameter (I) and mean residence time for all simulations combined. Each *symbol* represents and individual reef size and shape. *Grey shading*, colors, and *symbols* are as indicated in Figs. 4–6. The line is the regression pooled across all reef shapes (*rectangles triangles* and *kidneys*) and all circulation regimes (i.e., all unidirectional flow intensities (V m s^{-1}) and weak unidirectional and weak tidal (*wUwT*), weak unidirectional and strong tidal (*sUwT*), and strong unidirectional and strong tidal (*sUsT*))

indeed, a pair of persistent eddies rotating clockwise and anticlockwise were formed behind the obstacle (Fig. 2a). These circulation regimes also exhibited long residence times. Thus, this study supports the hypothesis that lee eddies act as a mechanism for retaining larvae close to their natal reef (Sponaugle et al. 2002). However, larval retention is enhanced only when eddies remain attached to the obstacle. Larger I values were found in simulations with tidal flows. The simulated tidal currents promote the displacement of lee eddies to the east and west sides of the reef during tidal reversal (Fig. 2b, c). These eddies were subsequently detached by jet currents, advected downstream and eventually dissipated. Residence times were shorter when tides were included (Fig. 7). Hence, the presence of transient eddies might also accelerate larval flushing by increasing diffusion, or by entraining particles in the rim of the eddy, provoking faster advection than that caused by the mean flow (Sandulescu et al. 2006). Snapshots of particle distribution over time show how, under unidirectional flows, particles circulate around prevailing lee eddies and have longer residence times (Fig. 3a, c) than particles trapped on eddies that, with the effect of tidal flows, detach from the reef and are advected downstream (Fig. 3b, d).

The Island Wake Parameter is designed to capture the characteristics of unidirectional flow past obstacles in shallow waters. Variations in the flow that approaches the obstacle, such as the effect of perpendicular tidal flows, or variations in reef shapes (i.e., the presence of a lagoon for the kidney shaped reefs), might well be expected to hinder the performance of the Island Wake Parameter. Therefore, we expected the relationship between residence times and I to vary amongst circulation regimes and reef shapes. A surprising finding of our study was that any such differences were sufficiently small that a single set of regression parameters explained most of the variation in residence times.

For a given unidirectional flow speed entering the model domain from the north, the presence of tides indirectly increases the speed of the southward flow within the model domain, in addition to directly producing oscillating East–West flows. Consequently, I is larger, compared to simulations with the same unidirectional flow magnitude (apparent in Figs. 5 and 7 by the rightward shift of points with tidal flows). However, the presence of tides did not markedly affect the relationship between I and residence time, apparent in the strong evidence against separate regression parameters for the different tidal regimes provided by the likelihood ratio test ($P > 0.6$), and the lack of a tendency for simulations with stronger tidal flows to lie consistently above or below simulations with weaker tides, for a given I (Fig. 5).

Nevertheless, the differences between parameter estimates for different unidirectional flow intensities and reef shapes were only marginally non-significant ($P = 0.06$ and 0.07, respectively), and there was some apparent structure to the residuals from the fits of the pooled models, both of which suggest that there may be small differences in how retention time responds to I that are consistent with our understanding of the physics of lee eddies.

Specifically, in the simulations with unidirectional flow, there is some evidence that stable eddies promote longer retention times when they occur in the presence of more intense flows. For instance, inspection of Fig. 4 suggests that, when I is in the range of 1-6, high unidirectional flow speeds tend to cause longer retention times than low flow speeds (light gray squares tend to lie below dark gray squares in this region). This might be because, in the presence of stable eddies, stronger flows produces stronger convergence at eddy rims, for a given I. Consistent with this interpretation, parameter a increases with flow speed, indicating higher predicted retention at $I = 1$ when regressions are conducted separately for different flow speeds (Table A1). However, because retention times are very similar across unidirectional flow speeds for large I, parameter b must also be higher for stronger flows, so that predicted retention for stronger flows converges with predicted retention for weaker flows at large I (Table A1).

The principal apparent difference between reef shapes is that regression parameter b is larger for the triangular and smaller for the kidney shaped reefs (Table A3). Signell and

Geyer (1991) studied the effect of flow past different geometric obstacles. They note that sharper obstacles, such as triangular shaped reefs, are more likely to induce eddy formation. We might expect this to provoke lower retention for such reefs if eddies are detached and advected downstream. Conversely, the lagoons formed by kidney shaped reefs might be expected to promote retention. Careful inspection of Fig. 6 provides some support for this, but only for intermediate I values. When $I \sim 1$, all reef shapes form stable eddies, and there is little difference in residence time suggesting that these eddies, rather than particle entrapment at the lagoon, is the main mechanism for retention. When $I \gg 1$, eddy shedding occurs regardless of reef shape, and again residence times are similar amongst shapes. In between, when tides are present, retention appears to be slightly lower for triangles (red, orange, and blue triangles generally appear below other shapes of the same color in Fig. 6), and higher for kidneys (red, orange, and blue open squares generally appear above other shapes of the same color in Fig. 6). The lower residence times for triangular reefs may occur because eddy shedding occurs more frequently at these reefs. Conversely, the higher residence times for kidney-shaped reefs may indicate that the retention in the reef lagoon becomes relatively more important as eddies become unstable, but before flows become strong enough to quickly transport larvae out of the lagoon.

Implications for self-recruitment

The present study shows that reef-scale circulation features lead to a wide range of retention times for an array of circulation regimes and reef morphologies reminiscent of the variety of shapes observed in nature. For self recruitment to occur, larvae must be retained at the natal reef until they acquire competence to settle. Many marine invertebrates are able to settle within a few days or even hours after spawning. Our study shows that substantial larval retention can occur over such time scales, for wide reefs of various shapes and circulation regimes. Indeed, the levels of larval retention modeled in this study may well substantially underestimate relative levels of self-recruitment relative to locally produced larvae which recruits elsewhere. For instance, coral larvae acquire settlement competence quickly and can retain it for extended periods of time (Connolly and Baird 2010). However, a larger proportion of retained larvae than flushed larvae would be likely to successfully recruit, because flushed larvae would have to be transported to another reef, and survive the journey. Even with strong unidirectional and tidal flows, retention can be high, particularly for reefs with semi-enclosed lagoons (Table 1). These findings indicate that reef-scale circulation features can facilitate self-recruitment for weak swimming larvae, or larvae that develop swimming capabilities at late developmental stages.

In addition, this study shows that the Island Wake Parameter is likely to be a useful tool for approximating larval retention, without the need to explicitly model local-scale three-dimensional circulation in the vicinity of reefs for a variety of reef shapes and prevailing circulation regimes. Specifically, a single regression between I and residence time (Eq. 3), explained 82% of the variation in residence time across all of our reef shapes and circulation regimes (Table 2). Moreover, separate regressions for different flow regimes suggested that the parameters characterizing the relationship between retention time and I change systematically across flow speed, indicating that it may be possible to comprehensively calibrate small differences in this relationship under different flow magnitudes, and thus explain an even higher proportion of the variation in retention time.

Estimating the effects of reef-scale, three-dimensional flows on larval retention in the vicinity of reefs is a significant problem for understanding, and predicting, larval dispersal patterns and the meta-population and evolutionary dynamics that they influence. This study identifies one approach to making such estimates in a simple, tractable way that does not require detailed, computationally intensive, and expensively calibrated reef-scale hydrodynamic models to be run for every location and time that is of interest.

Acknowledgments We are grateful to Dr. Mike Herzfeld for support running SHOC and initial ideas for the manuscript. We thank Dr. Peter Ridd for valuable comments during the development this work. Thanks to Geoff Millar and Simon Spagnol for IT support at AIMS. This research was funded by the Australian Research Council, James Cook University and the Australian Institute of Marine Science. P.C-H. received financial support from CONACyT and SEP (Mexico).

References

Barton ED (2001) Island wakes. In: Encyclopedia of ocean sciences. Elsevier, pp 1397-1403

Black KP, Gay SL (1987) Eddy formation in unsteady flows. J Geophys Res C 92:9514–9522

Bradbury IR, Snelgrove PVR (2001) Contrasting larval transport in demersal fish and benthic invertebrates: the roles of behaviour and advective processes in determining spatial pattern. Can J Fish Aquat Sci 58:811–823

Bricker JD, Nakayama A (2007) Estimation of far-field horizontal and vertical turbulent diffusion coefficients from the concentration field of a wastewater plume near the Akashi Strait. Environ Fluid Mech 7:1–22

Burchard HK, Peterson O, Rippeth TP (1998) Comparing the performance of the Mellor Yamada and the k turbulence models. J Geophys Res 103:10543–10554

Burgess SC, Kingsford MJ, Black KP (2007) Influence of tidal eddies and wind on the distribution of presettlement fishes around One Tree Island, Great Barrier Reef. Mar Ecol Prog Ser 341:233–242

Chia F-S, Buckland-Nicks J, Young CM (1984) Locomotion of marine invertebrate larvae: a review. Can J Zool 62:1205–1222
Condie SA, Andrewartha JR (2008) Circulation and connectivity on the Australian North West Shelf. Cont Shelf Res 28:1724–1739
Condie SA, Loneragan NR, Die DJ (1999) Modelling the recruitment of tiger prawns *Penaeus esculentus* and *P. semisulcatus* to nursery grounds in the Gulf of Carpentaria, northern Australia: implications for assessing stock-recruitment relationships. Mar Ecol Prog Ser 178:55–68
Connolly SR, Baird A (2010) Estimating dispersal potential for marine larvae: dynamic model applied to scleractinian corals. Ecology 91(12):3572–3583
Cowen RK, Paris CB, Srinivasan A (2006) Scaling of connectivity in marine populations. Science 311:522–527
Done TJ (1982) Patterns in the distribution of coral communities across the central Great Barrier Reef. Coral Reefs 1:95–107
Dong C, McWilliams JC (2007) A numerical study of island wakes in the Southern California Bight. Cont Shelf Res 27:1233–1248
Gerlach G, Atema J, Kingsford M, Black KP, Miller-Sims V (2007) Smelling home can prevent dispersal of reef fish larvae. Proc Natl Acad Sci USA 104:858–863
Glimour JP, Smith LD, Brinkman R (2009) Biannual spawning, rapid larval development and evidence of self-seeding for scelaractinian corals at an isolated system of reefs. Mar Biol 156:1297–1309
Griffin DA, Middleton JH, Bode L (1987) The tidal and longer-period circulation of Capricornia, Southern Great Barrier Reef. Aust J Mar Freshw Res 38:461–474
Hellberg ME, Burton RS, Neigel JE, Palumbi SR (2002) Genetic assessment of connectivity among marine populations. Bull Mar Sci 70:273–290
Herzfeld M, Waring JP, Margvelashvili N, Sakov P, Andrewartha J (2006) SHOC, Sparse Hydrodynamic Ocean Code V1.0 Scientific Manual, CSIRO Marine Research. http://www.emg.cmar.csiro.au/www/en/emg/software/EMS/hydrodynamics.html
Irisson J-O, LeVan A, De Lara M, Planes S (2004) Strategies and trajectories of coral reef fish larvae optimizing self-recruitment. J Theor Biol 227:205–218
James MK, Armsworth PR, Mason LB, Bode L (2002) The structure of reef fish metapopulations: modelling larval dispersal and retention patterns. Proc R Soc Lond B Biol Sci 269:2079–2086
Kingsford MJ, Leis JM, Shanks A, Lindeman KC, Morgan SG, Pineda J (2002) Sensory environments, larval abilities and local self-recruitment. Bull Mar Sci 70:309–340
Legrand S, Deleersnijder E, Hanert E, Legat V, Wolanski E (2006) High resolution, unstructured meshes for hydrodynamic models of the Great Barrier Reef, Australia. Estuar Coast Shelf Sci 68:36–46
Leys SP, Degnan BM (2001) Cytological basis of photoresponsive behaviour in a sponge larva. Biol Bull (Woods Hole) 201: 323–338
Marinone SG (2006) A numerical simulation of the two- and three-dimensional Lagrangian circulation in the northern Gulf of California. Estuar Coast Shelf Sci 68:93–100
Marinone SG, Ulloa MJ, Pares-Sierra A, Lavin MF, Cudney-Bueno R (2008) Connectivity in the northern Gulf of California from particle tracking in a three-dimensional numerical model. J Mar Syst 71:19–158
Moum JN, Caldwell DR, Stabeno PJ (1988) Mixing and intrusions in a rotating cold-core feature off Cape Blanco, Oregon. J Phys Oceanogr 18:823–833
Nahas EL, Jackson G, Pattiaratchi CB, Ivey GN (2003) Hydrodynamic modelling of snapper *Pagrus auratus* egg and larval dispersal in Shark Bay, Western Australia: reproductive isolation at a fine spatial scale. Mar Ecol Prog Ser 265:213–226
Neill SP, Elliott AJ (2004) Observations and simulations of an unsteady island wake in the Firth of Forth, Scotland. Ocean Dynam 54:324–332
Nozawa Y, Harrison PL (2008) Temporal patterns of larval settlement and survivorship of two broadcast-spawning acroporid corals. Mar Biol 155:347–351
Okubo A (1971) Oceanic diffusion diagrams. Deep-Sea Res 18: 789–802
Paris CB, Cowen RK (2004) Direct evidence of a biophysical retention mechanism for coral reef fish larvae. Limnol Oceanogr 49:1964–1979
Parslow JS, Gabric AJ (1989) Advection, dispersal and plankton patchiness on the Great Barrier Reef. Aust J Mar Freshw Res 40:403–419
Parslow JS, Herzfeld M, Hunter JR, Andrewartha JR, Sakov P, Waring J (2001) Mathematical modelling of the dispersal and fate of CES discharge from the Boyer Mill in the Upper Derwent Estuary: Results of Part B, final report CSIRO Div of Marine Research, Hobart, TAS, p 189
Pattiaratchi C, James A, Collins M (1986) Island wakes and headland eddies: A comparison between remotely sensed data and laboratory experiments. J Geophys Res C 92:783–794
Roberts CM (1997) Connectivity and management of Caribbean coral reefs. Science 278:1454–1457
Sale PF, Cowen RK, Danilowicz BS, Jones GP, Kritzer JP, Lindeman KC, Planes S, Polunin VCN, Russ GR, Sadovy JY, Steneck RS (2005) Critical science gaps impede use of no-take fishery reserves. Trends Ecol Evol 20:74–80
Sandulescu M, Hernandez-Garcia E, Lopez C, Feudel U (2006) Kinematic studies of transport across an island wake, with application to the Canary Islands. Tellus Ser A Dyn Meteorol Oceanogr 58A:605–615
Signell RP, Geyer WR (1991) Transient eddy formation around headlands. J Geophys Res C 96:2561–2575
Sponaugle S, Cowen RK, Shanks A, Morgan SG, Leis JM, Pineda J, Boehlert GW, Kingsford MJ, Lindeman KC, Grimes C, Munro JL (2002) Predicting self-recruitment in marine populations: biophysical correlates and mechanisms. Bull Mar Sci 70:341–375
Steneck RS (2006) Staying connected in a turbulent world. Science 311:480–481
Strathmann RR, Hughes TR, Kuris AM, Lindeman KC, Morgan SG, Pandolfi JM, Warner RR (2002) Evolution of local recruitment and its consequences for marine populations. Bull Mar Sci 70:377–396
Swearer SE, Shima JS, Hellberg ME, Thorrold SR, Jones GP, Robertson DR, Morgan SG, Selkoe KA, Ruiz GM, Warner RR (2002) Evidence of self-recruitment in demersal marine populations. Bull Mar Sci 70:251–271
Tang L, Sheng J, Hatcher BG, Sale PF (2006) Numerical study of circulation, dispersion, and hydrodynamic connectivity of surface waters on the Belize shelf. J Geophys Res C 111:C01003. doi:10.1029/2005JC002930
Taylor G (1954) The dispersion of matter in turbulent flow through a pipe. Proc R Soc Lond, A 223:446–468
Tomczak M (1988) Island wakes in deep and shallow water. J Geophys Res C 93:5153–5154
van Oppen MJH, Gates RD (2006) Conservation genetics and the resilience of reef-building corals. Mol Ecol 15:3863–3883
Visser AW (1997) Using random walk models to simulate the vertical distribution of particles in a turbulent water column. Mar Ecol Prog Ser 158:257–281
Walker SJ (1999) Coupled hydrodynamic and transport models of Port Phillip Bay, a semi-enclosed bay in south-eastern Australia. Mar Freshw Res 50:469–481

Whalan S, Ettinger-Epstein P, de Nys R (2008) The effect of temperature on larval pre-settlement duration and metamorphosis for the sponge, *Rhopaloeides odorabile*. Coral Reefs 27: 783–786

Willis BL, Oliver JK (1990) Direct tracking of coral larvae: Implications for dispersal studies of planktonic larvae in topographically complex environments. Ophelia 32:145–162

Wolanski E (1993) Facts and numerical artefacts in modelling the dispersal of Crown-of-thorns Starfish larvae in the Great Barrier Reef. Aust J Mar Freshw Res 44:427–436

Wolanski E, Hammer WM (1988) Topographically controlled fronts in the ocean and their biological influence. Science 241:177–181

Wolanski E, Pickard GL (1985) Long-term observations of currents on the Central Great Barrier Reef continental shelf. Coral Reefs 4:47–57

Wolanski E, Imberger J, Heron ML (1984) Island wakes in shallow coastal waters. J Geophys Res C 89:10553–10569

Wolanski E, Burrage D, King B (1989) Trapping and dispersion of coral eggs around Bowden Reef, Great Barrier Reef, following mass coral spawning. Cont Shelf Res 9:479–496

Wolanski E, Asaeda T, Tanaka A, Deleersnijder E (1996) Three-dimensional island wakes in the field, laboratory experiments and numerical models. Cont Shelf Res 16:1437–1452

Wolanski E, Brinkman R, Spagnol S, McAllister F, Steinberg C, Skirving W, Deleersnijder E (2003) Merging scales in models of water circulation: Perspectives from the Great Barrier Reef. In: Lakhan (ed) Advances in coastal modelling. Elsevier Science, pp 411-429